

Achieving the theoretical depairing current limit in superconducting nanomesh films

Ke Xu[†], Peigen Cao and James R. Heath*

Kavli Nanoscience Institute and Division of Chemistry and Chemical Engineering, California Institute of Technology, MC 127-72, Pasadena, CA 91125, USA

*: Corresponding author: JRH (heath@caltech.edu)

[†]: Current address: Department of Chemistry and Chemical Biology, Harvard University, 12 Oxford St., Cambridge, MA 02138

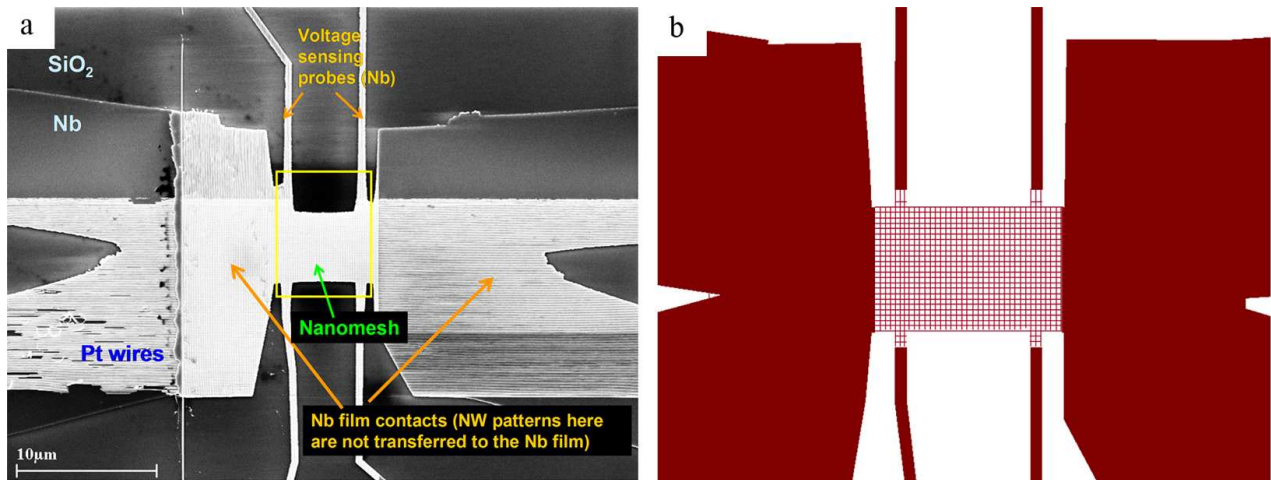
Supporting Information

Methods:

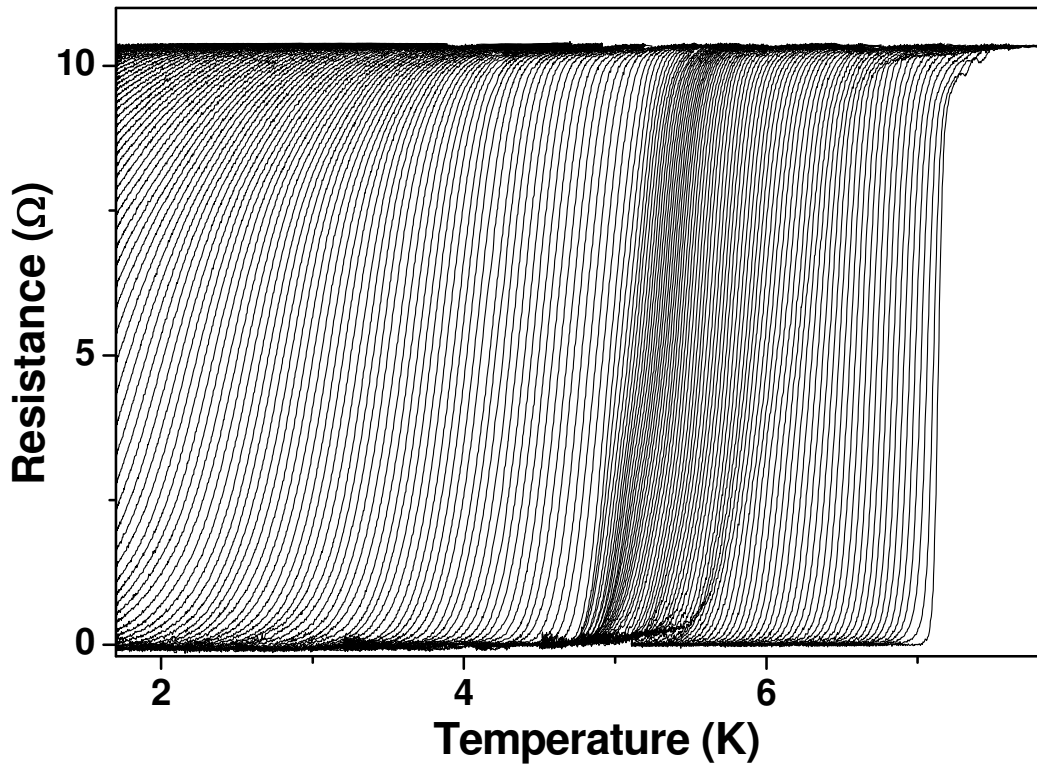
Superconducting Nb films were prepared in a Denton Vacuum Discovery 550 multi-cathode DC/RF magnetron sputter deposition system. Si substrates with a 300 nm thick SiO₂ top layer were cleaned in piranha solution (H₂SO₄/H₂O₂) and rinsed thoroughly with deionized water. Substrates were loaded onto a rotating stage and the chamber was first pumped down to 5×10⁻⁷ Torr (1 Torr ~ 133 Pa). The stage and the chamber were then baked at 300°C for 2 hours while continue pumping with a cryopump. In this way, a base pressure of 5.6×10⁻⁸ Torr was achieved when the chamber was cooled down to room temperature. Ultra-high purity argon (99.999%+) was introduced into the system as the sputtering gas at 16 sccm (standard cubic centimeters per minute) and kept at 2.5 mTorr. 11 nm of Nb was deposited at 0.9 nm/s by DC sputtering from a Nb target (99.96%, Plasmaterials, Livermore, CA, USA), after a 15-minute pre-sputtering with a shield between the substrates and the target to thoroughly clean the target surface. Without breaking the vacuum, 10 nm SiO₂ was immediately RF sputtered from a silicon dioxide target (99.995%, Kurt J. Lesker, Livermore, CA, USA) to cover Nb.

An array of 400 Pt SNAP nanowires (NWs) was first deposited onto the SiO₂-coated Nb film, with the width and periodicity of the NWs precisely controlled through the molecular beam epitaxy growth of the starting GaAs/Al_xGa_{1-x}As superlattice (IQE, Cardiff, UK) wafers^{22,23}. A second array of Pt NWs was then deposited on top of and perpendicular to the first array, thus forming a crossbar structure on the Nb film. E-beam lithography was used to pattern a 50 nm thick Al mask for sectioning the crossbar and the underlying Nb film into devices ~5 μm in width and ~5 μm in length with four-point contacts. For sectioning, a 40 MHz Unaxis SLR parallel-plate reactive ion etching (RIE) system was employed to completely remove all portions of Pt NWs and the underlying Nb that were not protected by the Al mask. An Ar plasma (20 sccm, 10 mTorr, 190 W) and a CF₄/He plasma (20/30 sccm, 5 mTorr, 40 W) were used to remove Pt and Nb, respectively. The Al mask was removed in diluted H₃PO₄ (1:10, 1 hour). Au/Ti (100/20 nm) contact pads for wirebonding were lithographically defined to contact the device. Before Au/Ti was deposited, the contact regions were briefly (3 seconds) dipped into a buffered oxide etch solution (6:1 of 40% NH₄F in water to 49% HF in water) to remove the SiO₂ top layer, so the Au/Ti contact pads were electrically connected to the Nb layer. In the final step, using the Pt crossbar structure as an etch mask, highly directional RIE (CF₄/He, 20/30 sccm, 5 mTorr, 40 W) converted the Nb film into a nanomesh device with contacts defined in the previous steps. Measurements were carried out in a pumped ⁴He system (Quantum Design MPMS-XL; base temperature 1.7 K) with standard DC techniques (Keithley 2400 SourceMeter and 2182 Nanovoltmeter).

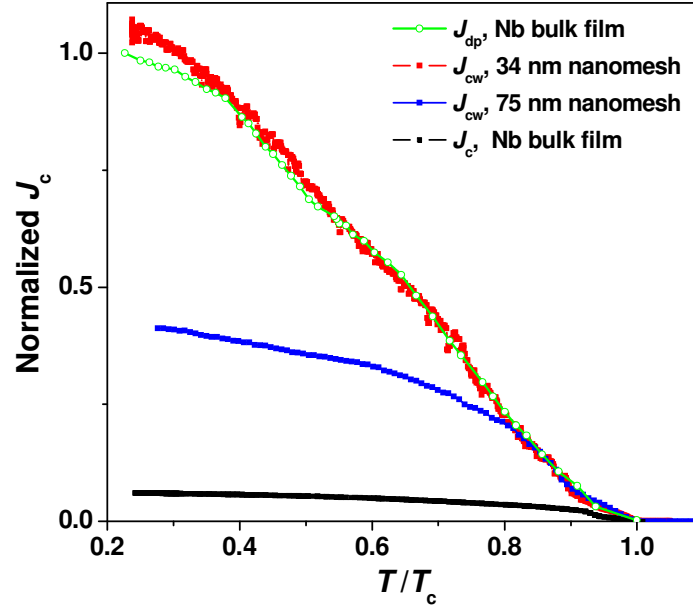
The architecture of the final nanomesh structure is illustrated in Supplementary Fig. 1a and 1b.



Supplementary Figure 1. The architecture of the nanomesh devices, and the structure of the Nb thin film (and Nb nanomesh) used in the experiments. (a): Scanning electron micrograph of a nanomesh device, with various of the relevant components labeled. The nanomesh is formed by using two perpendicularly oriented SNAP Pt nanowire arrays as masks. The outlined yellow region illustrates the region of the crossed SNAP nanowire arrays that were used as masks. In the regions away from the yellow box, the Nb has either been remove completely, or it is separated from the top Pt nanowire array by an insulating dielectric. (b): Illustration of the device structure, highlighting only the Nb components within the device. The nanomesh is represented by the cross-hatched pattern, and the 11 nm thick, continuous Nb film is represented by the solid maroon colored parts.



Supplementary Figure 2. R - T curves of the 34 nm pitch nanomesh collected at closely-spaced, fixed H (from 0 to 3.8 T in 0.02 T steps). The $T_c(H)$ curves discussed in the main text were obtained by determining the T_c of each individual R - T curve collected at fixed H . Due to the finite transition temperature width, a resistance criterion was used to determine T_c , i.e., T_c is defined as the temperature at which the measured resistance reaches the given criterion.



Supplementary Figure 3. Critical current density rescaled by T_c . The same experimental J_c-T results in Fig. 3a are rescaled in T by the T_c of each individual device. J_c is also rescaled by T_c to account for the overall linear dependency of J_{dp} on T .

When rescaled by T_c , a good agreement is again obtained between the J_c-T dependency of our 34 nm nanomesh and the previous $J_{dp}-T$ results. In the low-temperature limit, our result is slightly higher than the previous $J_{dp}-T$ result. The previous $J_{dp}-T$ result bends down for $T < \sim 0.3 T_c$ and thus slightly deviates from theory, indicating vortex flows may still be problematic at very high current levels, even for short pulses. In comparison, J_{dp} is robustly achieved in our continuous-current measurement of J_c . Supplementary Fig. 3 also demonstrates that for the 75 nm nanomesh, a good initial agreement between J_c and J_{dp} is observed for $T > \sim 0.8 T_c$, but J_c increasingly deviates from J_{dp} with decreasing T .